Improving residual robustness to noise for fault localization in a Y-shaped network

Abdelkarim Abdelkarim, Vincent Cocquempot, Mohamed Amine Atoui, Pierre Laly, Virginie Degardin

Improving residual robustness to noise for fault localization in a Y-shaped network

Abdel Karim Abdel Karim[1], Cocquempot Vincent[2], Atoui M. Amine, Laly Pierre[3], Degardin Virginie[3]

[1] *College of Engineering and Technology, American University of the Middle East, Egaila, 54200, Kuwait*
[2] *Univ. Lille, CNRS, Centrale Lille, UMR 9189 - CRIStAL, F-59000 Lille, France*
[3] *Univ. Lille, CNRS, Centrale Lille, Univ. Polytechnique Hauts-de-France, UMR 8520 - IEMN, F-59000 Lille, France*
e-mail: Abdel.Karim@aum.edu.kw, vincent.cocquempot@univ-lille.fr, amine.atoui@gmail.com, pierre.laly@univ-lille.fr, virginie.degardin@univ-lille.fr

Abstract: This paper aims at detecting soft faults, i.e. degradations, in Y-shaped communication networks and locating the faulty branch. The proposed method is based on the transmission coefficient (TC) between each source and the receivers. The estimation of the TC is performed online by power line communication technology through orthogonal frequency division multiplexing scheme. Then, a health indicator per receiver is computed and sent back to the source, which computes a set of structured residual signals for fault detection and localization. This method is validated by data collected on a laboratory test bench. To enhance the robustness of the residuals to noise, modified residuals are proposed. These new residuals are obtained by weighting the centered residuals by the Frequency Response Assurance Criterion. The experimental results confirm the robustness of the weighted residuals while maintaining their sensitivity to soft faults.

Keywords: Fault detection, Fault localization, Residual, Y-shaped communication network, Robustness, Frequency Response Assurance Criterion.

1. INTRODUCTION

Despite advances in wireless communication, cables are still prevalent in embedded systems like cars, trains, and planes, serving for energy transfer and data transmission. These cables tend to suffer from their own environment where moisture can cause water-tree degradation (Bulinski et al. (1986)), heat can cause thermal degradation, mechanical stresses can crack the cable isolation etc. The above degradations are qualified as *soft fault* provided that the transmission of data or energy is not affected. However, over time, they tend to develop into an *hard faults* where the cable degradation can lead to an open voltage circuit or to a short circuit which causes the system malfunction. Therefore, it is of prime importance to detect and localize a soft fault before it evolves to hard fault. Reflectometry methods, commonly used for this purpose, analyze reflected dedicated signals due to impedance discontinuities, resulting notably of faults, in the network. A review (Furse et al. (2020)) discusses these methods facing challenges such as small reflections detection due to signal attenuation and distortion, ambiguity in fault localization and blind spots (Auzanneau (2013)). Distributed reflectometry methods, requiring dedicated measurement instruments to separate transmitted and reflected signals, were proposed to address some of these challenges (Ben Hassen et al. (2015)). In such methods, several reflectometers are used and a data fusion algorithm is applied to obtain the final diagnostic result. Another approach for communication network monitoring, which is based on transferometry, is proposed in (Auzanneau (2016)). This approach was recently developed in (Abdel Karim et al. (2023)) where the network Transmission Coefficient (TC), i.e. frequency transfer function, $H(f)$, is estimated online by Power Line Communication (PLC) technology using Orthogonal Frequency Division Multiplexing (OFDM) scheme. The use of PLC for fault detection was studied in (Lallbeeharry et al. (2018), Huo et al. (2018), Yang et al. (2013)), where a reference TC and successive estimations of $H(f)$ are compared. The comparison method proposed in (Abdel Karim et al. (2021), Abdel Karim et al. (2022), Abdel Karim et al. (2023)) lies on the generation of health indicators and residual signals. An improvement of the latter work is proposed in this paper.

The main contributions of this paper are:

- Analyzing residual sensitivity to soft faults in a Y-shaped communication network, supported by theoretical proofs using health indicators derived from the network model.
- Generating a structured set of residuals for fault localization.
- Validating the method using real data collected from a laboratory test bench.

- Improving residual robustness to measurement and environmental noises by weighting the residuals with the Frequency Response Assurance Criterion index.

The paper is organized as follows. The transmission chain matrix method to model a Y-shaped network is briefly recalled in section 2. The health indicators used for fault detection and localization method are presented in section 3. Structured residuals are designed for fault localization in section 4. Experimental evaluation of the health indicators and the residuals is presented in section 5 and weighted residuals are proposed to enhance the robustness to noise. Conclusions and future work end this paper.

2. NETWORK MODELING

Health indicators and residuals will be defined in section 3. To prove their sensitivities to soft faults, the network is modeled in healthy and faulty cases.

2.1 Chain matrix model

In frequency domain, input and output voltage $V = [V_1; V_2]$ and current $I = [I_1; I_2]$ of a transmission line are linked by the transmission matrix (or chain matrix or ABCD matrix) (Esmailian et al. (2003)) as in (1).

$$\begin{bmatrix} V_1 \\ I_1 \end{bmatrix} = \begin{bmatrix} \mathbf{A} & \mathbf{B} \\ \mathbf{C} & \mathbf{D} \end{bmatrix} \times \begin{bmatrix} V_2 \\ I_2 \end{bmatrix} \tag{1}$$

$$\text{with } \begin{bmatrix} \mathbf{A} & \mathbf{B} \\ \mathbf{C} & \mathbf{D} \end{bmatrix} = \begin{bmatrix} ch(\gamma l) & Z_c \cdot sh(\gamma l) \\ \frac{1}{Z_c} \cdot sh(\gamma l) & ch(\gamma l) \end{bmatrix} = \Theta(l)$$

where, l is the length of the line, γ and Z_c are respectively the propagation constant and the characteristic impedance of the line. The chain matrices of an impedance Z in series and in parallel with a transmission line are given by

- Series impedance representation: $\Phi(Z) = \begin{bmatrix} 1 & Z \\ 0 & 1 \end{bmatrix}$
- Parallel impedance representation: $\Lambda(Z) = \begin{bmatrix} 1 & 0 \\ \frac{1}{Z} & 1 \end{bmatrix}$

A ramification can be replaced by an equivalent parallel impedance, Z_{eq}. This impedance can be computed by using (2):

$$Z_{eq} = \frac{\mathbf{a} \cdot Z_R + \mathbf{b}}{\mathbf{c} \cdot Z_R + \mathbf{d}} \tag{2}$$

where, $\mathbf{a}$, $\mathbf{b}$, $\mathbf{c}$ and $\mathbf{d}$ are the parameters of the ramification and Z_R is the impedance of the associated receiver located at the end of the ramification. A soft fault such as a bad connection in a transmission line or a local cable degradation can be represented by a series impedance according to Lallbeeharry et al. (2018) and Sommervogel (2020) where the value of this impedance Z_f indicates the severity of the fault.

2.2 Chain matrix for a Y-shaped network

A Y-shaped network, as shown in Fig. 1, consists of three ECU (electronic control unit), denoted ECU_i with $i \in \{0; 1; 2\}$, a node and three branches. A fault can occur in one of the three branches B_0, B_1 and B_2, so four cases, including the healthy case, of the network are explored in the following using the chain matrix model.
Each *ECU* can either play the role of a source or a receiver and they are considered line-matched ($Z_{ECU_0} = Z_{ECU_1} = Z_{ECU_2} = Z_c$). The network can be represented by cascaded distributed portions. Each portion of the network is represented by its appropriate transmission chain matrix. Detailed instructions for determining the chain matrix between each source to its corresponding receivers in the four cases of the network are provided in (Abdel Karim et al. (2021)).

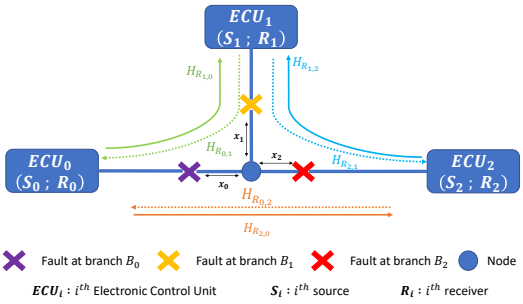

Fig. 1. Y-shaped network.

2.3 Transmission coefficient of a Y-shaped network

The transmission coefficient (TC) between a source S_k and a receiver R_i can be computed in each of the aforementioned cases by using (3) under the condition of matched impedance Bahl (2009).

$$H_{R_{i,k}}(f) = \frac{2 \cdot V_2}{V_1 + Z_s \cdot I_1} = \frac{2}{\mathbf{A} + \frac{\mathbf{B}}{Z_c} + \mathbf{C} \cdot Z_c + \mathbf{D}} \tag{3}$$

where Z_s is the impedance at the source.

3. FAULT DETECTION AND LOCALIZATION METHOD

The fault detection and localization method is based on a health indicator which is deduced from the analytical form of the transmission coefficients (TCs), $H_{R_{i,k}}(f)$, calculated between the source S_k and the two receivers R_i of the network shown in Fig. 1 with $i, k \in \{0; 1; 2\}$ and $i \neq k$.

3.1 Definition of the health indicator

The health indicator, $I_{R_{i,k}}(f)$, computed locally for the frequency f, at the receiver R_i when S_k is the source, is:

$$I_{R_{i,k}}(f) = \frac{\left|H_{R_{i,k}}^{Reference}(f)\right|}{\left|H_{R_{i,k}}(f)\right|} - 1 \quad \forall\, f \in BW \tag{4}$$

where $\left|H_{R_{i,k}}^{Reference}(f)\right|$ is the module of the network transmission coefficient between S_k and R_i in no-fault (healthy) nominal (no noise) situation, which is supposed to be known. $\left|H_{R_{i,k}}(f)\right|$ is the module of the transmission coefficient that is estimated online and BW is the bandwidth that is chosen accordingly to the application.

3.2 Evaluation and comparison of the health indicators

The expressions of the health indicators are derived from the expressions of the TCs (Abdel Karim et al. (2021)). The following results are obtained:

- Healthy network case: In a healthy nominal case, the two computed health indicators equal zero:

$$I_{R_{1,0}}(f) = I_{R_{2,0}}(f) = 0 \quad (5)$$

- Faulty source branch B_0: In the case where the fault is located at the branch B_0, the health indicators are proved to be equal:

$$I_{R_{1,0}}(f) = I_{R_{2,0}}(f) \neq 0 \quad (6)$$

$$I_{R_{1,0}}(f) = \left| \frac{6 \cdot Z_c + Z_f \cdot (3 + e^{-2\gamma x_0})}{6 \cdot Z_c} \right| - 1$$

where x_0 is the distance between the fault position and the node, Z_f denotes the impedance of the fault.

- Faulty receiver branch B_i: The expressions of the health indicators, when a fault is located at the branch B_i ($i \in 1; 2$), are obtained using (4) and the expressions of the transmission coefficients are

$$I_{R_{i,0}}(f) = \left| \frac{6 \cdot Z_c + 3 \cdot Z_f + Z_f \cdot e^{-2\gamma x_i}}{6 \cdot Z_c} \right| - 1 \quad (7)$$

A signature matrix as shown in Table 1 can be constructed for a Y-shaped network. This matrix is based on the theoretical expressions of the health indicators in the nominal (no noise) case. In the practical case, noises will influence the health indicator. Thus, a decision method should be used to identify the healthy or faulty case.

Table 1. Y-shaped network signature matrix of the Health Indicators.

Healthy network	Faulty B_0	Faulty B_1	Faulty B_2
$I_{R_{1,0}} = I_{R_{2,0}} = 0$	$I_{R_{1,0}} = I_{R_{2,0}} = 0$	$I_{R_{1,0}} \neq I_{R_{2,0}}$	$I_{R_{1,0}} \neq I_{R_{2,0}}$
$I_{R_{0,1}} = I_{R_{2,1}} = 0$	$I_{R_{0,1}} \neq I_{R_{2,1}}$	$I_{R_{0,1}} = I_{R_{2,1}} = 0$	$I_{R_{0,1}} \neq I_{R_{2,1}}$
$I_{R_{0,2}} = I_{R_{1,2}} = 0$	$I_{R_{0,2}} \neq I_{R_{1,2}}$	$I_{R_{0,2}} \neq I_{R_{1,2}}$	$I_{R_{0,2}} = I_{R_{1,2}} = 0$

4. FAULT LOCALIZATION BASED ON STRUCTURED RESIDUALS

Residuals are introduced to compare the health indicators between them.

4.1 Definition of the residuals

Definition 1. The residual r_k is defined as the mean value of the Manhattan distance between each pair of health indicators.

$$r_{k,ij} = \frac{1}{N_f} \sum_f |I_{R_{i,k}}(f) - I_{R_{j,k}}(f)| \quad with\ f \in BW \quad (8)$$

where BW is the frequency bandwidth of interest and N_f is the number of frequency values in BW. The residual r_k is computed at the source S_k and the health indicators, $I_{R_{i,k}}(f)$ and $I_{R_{j,k}}(f)$, are computed respectively at the receivers R_i and R_j.

Due to the presence of noise and its nonlinear influence, the residual $r_{k,ij}$ will be non zero even in the no fault situation. To make the decision easier, a centered residual is computed by subtracting its mean value in healthy situation to its actual value.

Definition 2. The centered residual, $r^c_{k,ij}$, is defined as :

$$r^c_{k,ij} = r_{k,ij} - \frac{1}{N_H} \cdot \sum_n r^{H_n}_{k,ij} \quad (9)$$

where $r^c_{k,ij}$ denotes the centered residuals, N_H is the number of healthy estimates of the transmission coefficients, $r^{H_n}_{k,ij}$ corresponds to the n^{th} residual in healthy case.

Table 2 presents the signature matrix of the residuals (Gertler (1992)).

Table 2. Residuals' signature matrix for a Y-shaped network.

r_k	Healthy	Faulty B_0	Faulty B_1	Faulty B_2
r_0	0	0	1	1
r_1	0	1	0	1
r_2	0	1	1	0

4.2 Representation of the residuals

The three centered residuals, r_0, r_1 and r_2, can be represented in the residual space as seen in Fig 2.

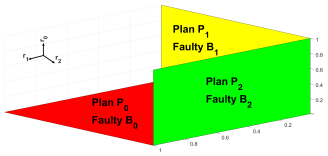

Fig. 2. Residual space representation.

The residual space is formed of three planes:

- The plane P_0 formed by r_1 and r_2.
- The plane P_1 formed by r_0 and r_2.
- The plane P_2 formed by r_0 and r_1.

Two cases of the network are explored :

Healthy network If the network is fault free, the three residuals are null ($r_0 = r_1 = r_2 = 0$). This case corresponds to a point at the center $(0; 0; 0)$.

Faulty B_i If the fault is located at the branch B_i, only one residual is assumed to be zero ($r_i = 0$) and the other two are non-zero ($r_j \neq 0$ and $r_k \neq 0$, with i, j and $k \in \{0; 1; 2\}$ and $i \neq j \neq k$). This case corresponds to a point in the P_i plane.

In summary, to detect and locate the faulty branch, the computed residuals will be plotted in the residuals space. If the point is not at the center $(0; 0; 0)$, a soft fault is detected. If the point belongs to the plane P_i, then the fault is at the branch B_i. Moreover, as it may be shown experimentally, the distance to the center $(0; 0; 0)$ is a function of the severity of the soft fault.

5. EXPERIMENTAL EVALUATION OF THE HEALTH INDICATORS AND THE RESIDUALS

5.1 Laboratory test bench

To validate our proposed soft fault detection and localization method, a laboratory test bench was set up. The test bench is a Y-shaped network similar to the one

shown in Fig. 1. The three branches are connected with a node. The installed cables are unshielded twisted pair cables of type DRB 18 with a characteristic impedance of nearly 120 Ω surrounded by 6 AWG14 single wires (single wires are not loaded). A fault represented by a $Z_f \in \{5\Omega\ ; 10\Omega\ ; 47\Omega\ ; 100\Omega\}$ can be easily inserted in series and removed in the three different positions shown in Fig. 1. The length of the branches B_0, B_1 and B_2 are respectively $l_0 = 4.25\ m$, $l_1 = 5\ m$ and $l_2 = 5.1\ m$. The distance between the fault positions and the node in each branch is $x_0 = 1.75\ m$, $x_1 = 2.5\ m$ and $x_2 = 1.5\ m$.
A Vector Network Analyser (VNA E5071C) is used to inject a signal into the network and to estimate the TCs between each source and each two end lines in the frequency band of $[0.1 : 100]\ MHz$ with 1601 frequency components (Inter Frame BandWidth, $IFBW = 10\ kHz$). Since the input and outputs of the VNA have an impedance of 50 Ω different to that of the lines, 3 baluns are used to match the network to the measurement instruments. A white Gaussian noise with a power of P_{noise} is added to the received signal at each end of the line to approach real conditions as in a vehicle and to test the sensitivity of the proposed residuals.

5.2 Transmission coefficients estimation

Four network cases are considered. The healthy case, where the TCs between each pair of baluns are estimated when the network is free from faults with a Signal to Noise Ratio (SNR) of 50 dB. The other three cases, where the TCs between each pair of baluns are estimated when the fault is inserted at one of the three branches B_0, B_1 and B_2. In each of the faulty cases, different impedance values, Z_f, representing the severity of a fault are inserted in series. A total of 13 different situations are considered where each situation is represented by a subset of 100 observations.

5.3 Computed health indicators

The health indicators are computed using the estimations of the TCs in different situations and plotted in function of the frequency. A rough comparison is first made which shows the validity of the theoretical characteristics.

Healthy network case: In Fig. 3, the health indicators are shown when the network is fault-free. Recalling table 1, theoretically each pair of health indicators in the healthy network are supposed to be equal to zero ($I_{R_{1,0}}(f) = I_{R_{2,0}}(f) = 0$, $I_{R_{0,1}}(f) = I_{R_{2,1}}(f) = 0$ and $I_{R_{0,2}}(f) = I_{R_{1,2}}(f) = 0$). In a real application as seen in Fig. 3, all indicators vary around zero due to the noise.

Faulty B_0 case: In Fig. 4, the health indicators are presented for the case of a 5 Ω resistor inserted in series at the B_0 branch. As seen in this figure, the first pair of health indicators are globally superimposed thus they can be considered as similar ($I_{R_{1,0}}(f) = I_{R_{2,0}}(f)$). The two other pairs are different from each other ($I_{R_{0,1}}(f) \neq I_{R_{2,1}}(f)$ and $I_{R_{0,2}}(f) \neq I_{R_{1,2}}(f)$).

Faulty B_2 case: In Fig. 5, the health indicators are presented for the case of a 47 Ω resistor inserted in series at the B_2 branch. As seen in this figure, the third pair of health indicators are globally superimposed thus they can be considered as similar ($I_{R_{0,2}}(f) = I_{R_{1,2}}(f)$). The two other pairs are different from each other ($I_{R_{0,1}}(f) \neq I_{R_{2,1}}(f)$ and $I_{R_{1,0}}(f) \neq I_{R_{2,0}}(f)$).

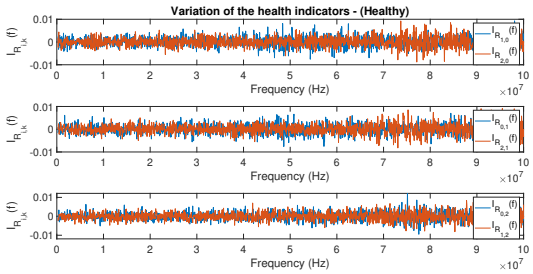

Fig. 3. Health indicators in the healthy case.

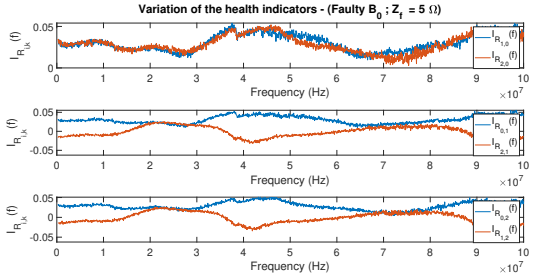

Fig. 4. Health indicators with a 5Ω resistor inserted at B_0.

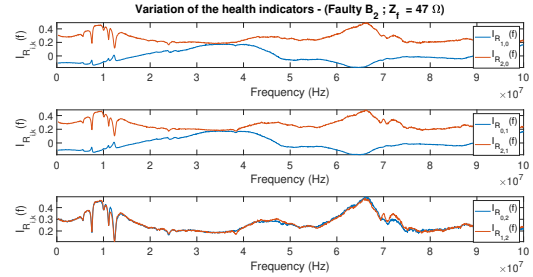

Fig. 5. Health indicators with a 47Ω resistor inserted at B_2.

5.4 Comparison of the health indicators using the residuals

Using the previous measurements, the 3 centered residuals are computed for each observation. The centered residuals, r_0, r_1 and r_2, are represented in a 3D space in Fig. 6. Each point represents an observation (i.e. the three centered

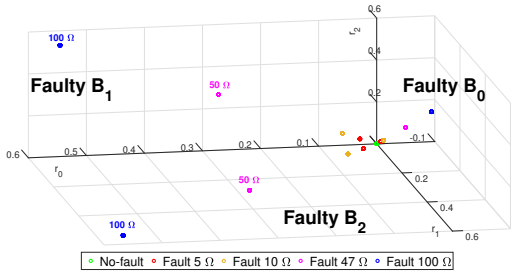

Fig. 6. Representation of the computed centered residuals (1300 observations, where each observation is composed of 3 residual values).

residual values) and each subset of 100 observations forms a cluster of 100 points. Thus, a total of $13 \times 100 = 1300$ observations are plotted. The green cluster, representing the healthy case of the network, is centered at (0; 0; 0). The other colors correspond to different faulty situations. From the plane to which the cluster belongs, the faulty branch can be isolated as expected. The position of the cluster depends on the severity of the fault : the greater the severity of the soft fault, the further the cluster is from the center. Due to page limitation, only the faulty B_0 case is detailed in the following. The B_1 and B_2 faulty cases have similar characteristics in their respective planes.

Faulty B_0 case. The centered residuals are presented in Fig. 7 and Fig. 8 in the planes P_0 and P_2. Red clusters represent the residuals in the B_0 faulty cases of the network with the four different severities of the fault Z_f.

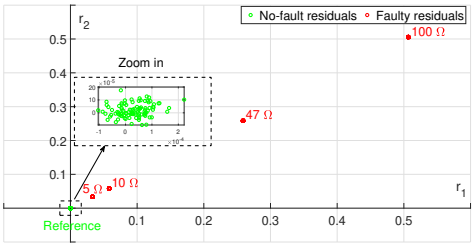

Fig. 7. Variation of the residuals. (plane P_0, faulty B_0)

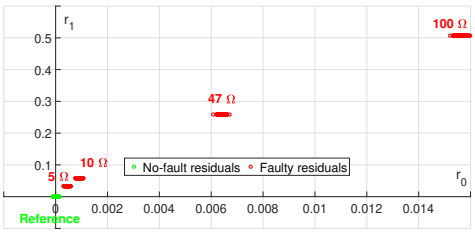

Fig. 8. Variation of the residuals. (plane P_2, faulty B_0)

In the plane P_0, the green cluster is around (0;0). The red clusters are distant from the healthy green cluster. These distances increase with the severity of the fault Z_f.
In the plane P_2, the projections of the residuals on the r_0 axis are very small, compared to the projections on the other axes. Theoretically, these values should be exactly zero as it was shown in section 4. The small values are due to measurement and environment noises. To improve the robustness to noise while keeping the sensitivity of these residuals, modified residuals are proposed in the following.

5.5 Improving the robustness of the residuals

In order to improve the robustness to noise, modified residuals are proposed in the following. These new residuals, called in the following as *practical residuals*, are obtained by weighting the centered residuals by a factor which depends on the similarity between two signals in the frequency domain. Let first give a definition of the Frequency Response Assurance Criterion (FRAC).

Definition 3. The FRAC reported in (Pascual et al. (1997)) is one of the most known correlation metrics used to test the similarity between two signals in the frequency domain. It is defined as

$$FRAC(X,Y) = \frac{|\sum_k X(f_k) \cdot Y^*(f_k)|^2}{\sum_k X(f_k) \cdot X^*(f_k) \sum_k Y(f_k) \cdot Y^*(f_k)} \quad (10)$$

where X and Y denote the two signals to be compared. J^* denotes the conjugate of J and $|J|$ is the module of J. f_k denotes the frequency of the k^{th} frequency component.

The FRAC index quantifies the existence or absence of a relationship between two signals. It provides a value between 0 and 1, where 1 denotes a perfect correlation between the compared signals and 0 denotes a no correlation situation or a significant difference between the two compared signals. This metric may be used to compare the deterministic values of the health indicators $I_{R_{i,k}}(f)$ in presence of noise.

As mentioned earlier, two cases may occur :

- If the health indicators, $I_{R_{i,k}}(f)$ and $I_{R_{j,k}}(f)$ are similar, $FRAC(I_{R_{i,k}}(f), I_{R_{j,k}}(f))$ equals theoretically 1.
- If the health indicators, $I_{R_{i,k}}(f)$ and $I_{R_{j,k}}(f)$ are different from each other, $FRAC(I_{R_{i,k}}(f), I_{R_{j,k}}(f))$ is theoretically equal to 0.

Definition 4. Practical residuals are obtained by weighting the centered residuals (9) by the complement to 1 of the FRAC index (10) of the 2 corresponding health indices.

$$wr_k = (1 - FRAC(I_{R_{i,k}}, I_{R_{j,k}})) \cdot r_k^c \quad (11)$$

In a healthy network, the FRAC indices are close to 1 so the healthy residuals remain quite the same. In a faulty network, if the two compared health indicators are similar, the residual is multiplied by a weight whose value is near zero which results in a new residual closer to zero. The robustness of the residual is enhanced. However, if the two compared health indicators are dissimilar, the residual is multiplied by a factor near one which results in a new value of the residual which remains quite the same to the initial value. The sensitivity to the fault is very slightly affected. The weighting factor $(1 - FRAC)$ is used to adjust the residuals that is influenced by noise.

A comparison between the centered residuals and the practical (weighted) residuals is made in the following section to show that the robustness of the new residuals is enhanced, while keeping the fault sensitivity.

5.6 Comparison between the 2 residuals using test bench measurements

The same measurements as above are used in the following. The residuals are computed for each case of the network. Due to page limitation, only the faulty B_0 case is presented. The results are similar for the other cases.

Faulty B_0. The centered residuals and practical (weighted) residuals are presented in Fig. 9, Fig. 10 and Fig. 11 in the planes (resp.) P_0, P_1 and P_2 in the presence of a fault in B_0. Several clusters are added to the initial figures presented in section 5.4, the yellow cluster representing the weighted residuals in the healthy case and the magenta clusters representing the weighted residuals in the faulty cases of the network with four different severities of the fault Z_f.

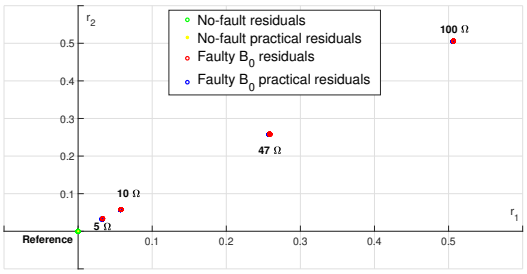

Fig. 9. Residuals and weighted residuals. (plane P_0)

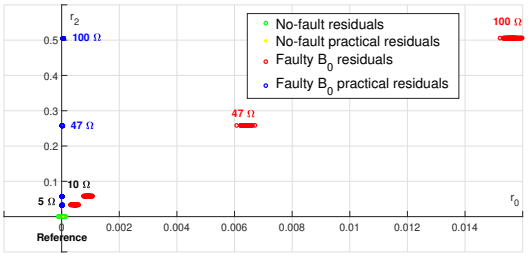

Fig. 10. Residuals and weighted residuals. (plane P_1)

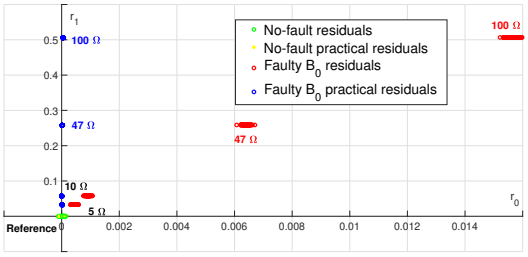

Fig. 11. Residuals and weighted residuals. (plane P_2)

The robustness of the residual is clearly enhanced since the projection of the practical residuals to the r_0 axis is now very close to zero. The same results and conclusions are obtained for all the other faulty cases.

6. CONCLUSIONS AND FUTURE WORK

This paper proposes a method to improve decision for fault detection and localization in Y-networks using PLC technology. Residuals based on health indices are used to compare the frequency response of the network to a reference response under no fault hypothesis. A real test bench is used to validate our approach. Enhanced residuals are obtained by weighting the initial residuals by a similarity index, the so-called FRAC between the compared health indices. It is shown that the robustness of the new residuals to measurement and external disturbances is greatly improved. Further work will be devoted to identify the type and severity of the detected fault.

REFERENCES

Abdel Karim, A.K., Atoui, M.A., Degardin, V., Laly, P., and Cocquempot, V. (2023). Bus network decomposition for fault detection and isolation through power line communication. *ISA Transactions*, 137, 492–505.

Abdel Karim, A.K., Atoui M, A., Degardin, V., and Cocquempot, V. (2021). Fault detection and localization in y-shaped network through power line communication. In *5th Int. Conf. on Control and Fault-Tolerant Systems (IEEE SysTol)*, 103–108.

Abdel Karim, A.K., Degardin, V., and Cocquempot, V. (2022). Sensitivity analysis of residuals for soft fault monitoring in y-shaped networks. In *2022 International Conference on Control, Automation and Diagnosis (ICCAD)*, 1–6.

Auzanneau, F. (2013). Wire troubleshooting and diagnosis: Review and perspectives. *Progress In Electromagnetics Research B*, 49, 253–279.

Auzanneau, F. (2016). Transferometry: A new tool for complex wired networks diagnosis. *Progress In Electromagnetics Research B*, 70, 87–100.

Bahl, I. (2009). *Fundamentals of RF and microwave transistor amplifiers*. John Wiley & Sons.

Ben Hassen, W., Auzanneau, F., Incarbone, L., Pérès, F., and Tchangani, A.P. (2015). Distributed sensor fusion for wire fault location using sensor clustering strategy. *Int. Journal of Distributed Sensor Networks*, 11(4).

Bulinski, A.T., Bamji, S.S., and Densley, R.J. (1986). The effects of frequency and temperature on water tree degradation of miniature xlpe cables. *IEEE Transactions on Electrical Insulation*, EI-21(4), 645–650.

Esmailian, T., Kschischang, F.R., and Glenn Gulak, P. (2003). In-building power lines as high-speed communication channels: channel characterization and a test channel ensemble. *International Journal of Communication Systems*, 16(5), 381–400.

Furse, C.M., Kafal, M., Razzaghi, R., and Shin, Y.J. (2020). Fault diagnosis for electrical systems and power networks: A review. *IEEE Sensors Journal*, 21(2), 888–906.

Gertler, J. (1992). Structured residuals for fault isolation, disturbance decoupling and modelling error robustness. *IFAC Proceedings Volumes*, 25(4), 15–23.

Huo, Y., Prasad, G., Lampe, L., and Leung, V.C. (2018). Cable health monitoring in distribution networks using power line communications. In *IEEE International Conference on Communications, Control, and Computing Technologies for Smart Grids*, 1–6. Aalborg, Denmark, Oct. 2018.

Lallbeeharry, N., Mazari, R., Dégardin, V., and Trebosc, C. (2018). Plc applied to fault detection on in-vehicle power line. In *IEEE International Symposium on Power Line Communications and its Applications*, 1–5. Manchester, UK, April 2018.

Pascual, R., Golinval, J.C., and Razeto, M. (1997). A frequency domain correlation technique for model correlation and updating. *Proceedings of SPIE: The International Society for Optical Engineering*.

Sommervogel, L. (2020). Various models for faults in transmission lines and their detection using time domain reflectometry. *Progress In Electromagnetics Research C*, 103, 123–135.

Yang, F., Ding, W., and Song, J. (2013). Non-intrusive power line quality monitoring based on power line communications. In *2013 IEEE 17th Int. Symp. on Power Line Communications and its Applications*, 191–196.